Power-electronic-interface topology for MEMS energy harvesting with multiple transducers

IOP Conf. Series: Journal of Physics: Conf. Series **1052** (2018) 012074 doi:10.1088/1742-6596/1052/1/012074

Power-electronic-interface topology for MEMS energy harvesting with multiple transducers

Binh Duc Truong[1,2], Cuong Phu Le[1], Einar Halvorsen[1] and Shad Roundy[2]

[1] Department of Microsystems, University College of Southeast Norway, Campus Vestfold, Raveien 215, 3184 Borre, Norway.
[2] Department of Mechanical Engineering, University of Utah, 50 S Central Campus Drive, Salt Lake City, UT 84112, USA.

E-mail: shad.roundy@utah.edu

Abstract. Based on circuit simulations, this paper investigates a concept for a power electronic interface circuit for MEMS electrostatic energy harvesters. Two ordinary overlap-varying transducers are first electrically configured as a symmetric voltage doublers which enables the device to self-start from an initially low bias. The harvesting system is then reconfigured to couple with a buck-boost DC-DC converter in order to maximize the power delivered to an electronic load. The losses of electronic components due to diode voltage drop and parasitic resistance of inductors are taken into account for a feasibility investigation. Dependence of the maximum output power on inductance and switching frequency is explored.

1. Introduction

Development of standalone wireless sensors and implantable electronic devices over the past decades has been in a fast pace [1, 2]. Current portable electronics requires the use of batteries for supplying electrical energy [3]. They don't have sufficient energy density to last for a long time and may pose a toxic threat in implanted sensors [4]. Energy harvesting from vibration is one means for replacing batteries [5]. This energy conversion typically uses either piezoelectric, electromagnetic or electrostatic transduction even though some alternatives such as triboelectricity [6] and magnetostriction [7] also have been considered. In this paper, we focus on electrostatic harvesters due to their compatibility with microelectronics [8] and their suitability for microfabrication and miniaturization.

The power electronic interface forms an essential component in an energy harvesting system. Interface circuits ranging from simple passive diode rectification to complicated active-switch converters with smart control units have been reported in the literature. The primary aim is to maximize harvested power or harvester effectiveness [9–11]. In a recent work, an interesting configuration of Bennet's doubler composed of capacitors and diodes was proposed by de Queiroz [12]. When the output voltage across the storage capacitor is saturated [13], vibration energy is no longer scavenged. Therefore, for continued scavenging in a real system, control circuitry must reconfigure the system at this point. Several conceivable solutions were presented such as buck [14] and reversible buck-boost [15] converters. However, the former circuit is not able to synthesize an optimum load, which makes it hard to optimize the harvested power.

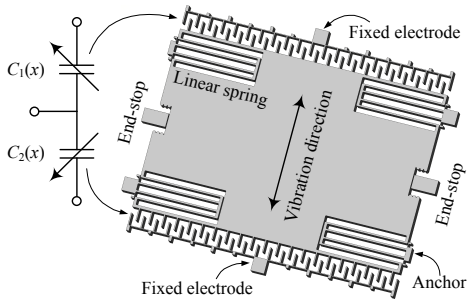

Figure 1: Schematic of the anti-phase overlap-varying electrostatic energy harvester.

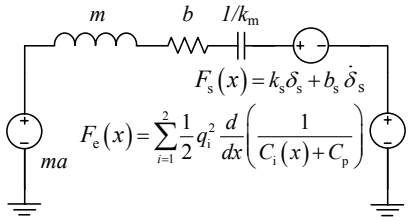

Figure 2: Equivalent circuit for mechanical domain.

Table 1: Model parameters

Parameters	Value
(a) *Device design*	
Proof mass, m	0.739 mg
Spring stiffness, k_m	16.41 N/m
Thin-film air damping, b	2.5e-5 Ns/m
Nominal overlap, x_0	110 μm
Nominal capacitance, C_0	15.16 pF
Parasitic capacitance, C_p	5.5 pF
Contact stiffness, k_s	3.361 MN/m
Impact damping, b_s	0.435 Ns/m
Max displacement, X_{max}	101.5 μm
(b) *Interface circuit*	
Biasing capacitor, C_b	1 nF
Storage capacitor, C_R	20 nF
ON resistance of SW, R_s	2 Ω
Inductance, L	150 μH
Inductor resistance, R_{sL}	45 kΩ/H
Output capacitance, C_S	1 μF
Load, R_L	5 MΩ

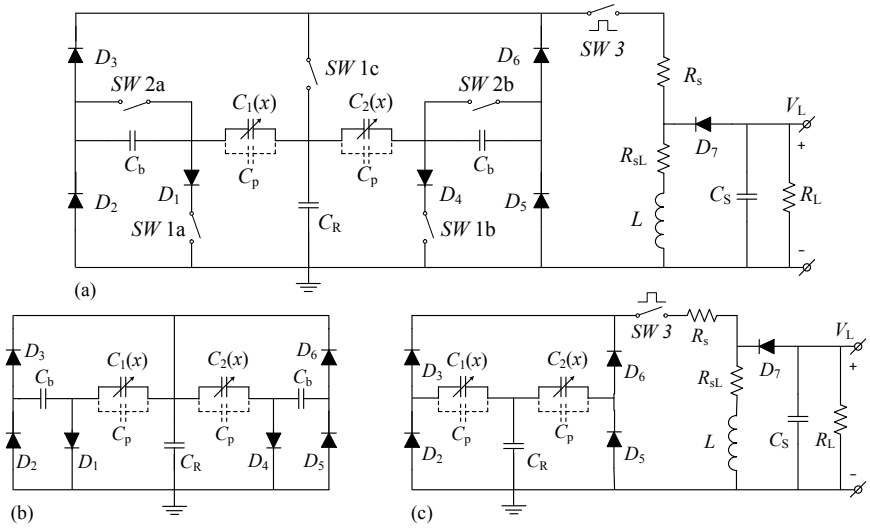

Figure 3: (a) Power electronic interface constructed by symmetrical voltage doubler and buck-boost converter and its corresponding operations when (b) *SW* 1abc [C], *SW* 2ab and *SW* 3 [O] and when (c) *SW* 1abc [O], *SW* 2ab [C] and *SW* 3 controlled by duty cycle. Notation: *SW* - switch, [C] - closed and [O] - open.

Many switches need to be continuously controlled in the latter topology which adds to the power consumption.

An advantage of the voltage doubler configuration is the potential to bootstrap itself from a low initial bias. In addition, a full-bridge rectifier and a buck-boost converter without an input filter capacitor may provide a resistive input impedance by tuning the duty cycle [16]. Based on circuit simulation, this contribution introduces an alternative interface circuit that combines those two interesting aspects. The question of how to optimize the ability of the processing circuit to harvest the maximum available output power is also an important issue in our study.

2. Energy harvester lumped-model

An anti-phase overlap-varying electrostatic energy harvester is considered for this investigation. Such a capacitor structure is shown in Figure 1. The proof mass m is suspended by four folded-beam springs with total linear stiffness k_m, while its motion is damped by a parasitic damping b and its maximum displacement X_{max} is defined by mechanical end-stops. The potential contact between the mass and the end-stops at sufficiently high accelerations are represented by the impact force F_s. The mass is also subject to the electrostatic force F_e generated by the

transducers. This system is governed by the following differential equation

$$m\ddot{x} + b\dot{x} + k_{\mathrm{m}}x + F_{\mathrm{e}}\big(x\big) + F_{\mathrm{s}}\big(x\big) = ma \tag{1}$$

where $ma = mA\cos\big(\omega t\big)$ is the fictitious force with angular frequency ω. The two forces F_{e} and F_{s} are

$$F_{\mathrm{e}}\big(x\big) = \frac{1}{2}q_1^2\frac{\mathrm{d}}{\mathrm{d}x}\frac{1}{C_1\big(x\big)+C_{\mathrm{p}}} + \frac{1}{2}q_2^2\frac{\mathrm{d}}{\mathrm{d}x}\frac{1}{C_2\big(x\big)+C_{\mathrm{p}}}, \tag{2}$$

and

$$F_{\mathrm{s}}\big(x\big) = k_{\mathrm{s}}\delta + b_{\mathrm{s}}\dot{\delta} \tag{3}$$

where q_1 and q_2 are the charges on the transducers 1 and 2 respectively, $C_{1/2} = C_0\big(1 \pm \frac{x}{x_0}\big)$, C_{p} is stray capacitance in parallel with $C_{1/2}$, k_{s} is the end-stop stiffness, b_{s} is the impact damping and $\delta = |x| - X_{\max}$ is the relative displacement between the proof mass and the end-stops during impact. The equivalent circuit for the mechanical domain is depicted in Figure 2. Parameters of the design are listed in Table 1a.

3. Power electronic interface

Figure 3a shows how the harvester is coupled to the proposed circuit. Operation of the harvesting system can be divided into two schemes as presented in Figure 3b and 3c. At the beginning, *SW* 1*a*, 1*b* and 1*c* closed, *SW* 2*a*, 2*b* and 3 open, the two transducers are initially configured as a symmetric voltage doubler. The storage capacitor C_{R} is pre-charged to a voltage of V_0. For sufficiently high V_0, the voltage accumulated on C_{R}, namely $V_{C_{\mathrm{R}}}$, initially increases. After a certain number of cycles, steady state is achieved and $V_{C_{\mathrm{R}}}$ is maintained constant at $V_{C_{\mathrm{R}}} = V_{\mathrm{sat}}$. The states of switches 1*a*, 1*b*, 1*c*, 2*a* and 2*b* are then reversed. The energy harvesters are now connected to a buck-boost DC-DC converter without input filter capacitor and with diodes D_2, D_3, D_5 and D_6 functioning as a rectifier. Simultaneously, the transducers are primed by the "bias" voltage V_{sat} while C_{R} is acting as an energy storage. The electronic load is represented by the resistor R_{L} in parallel with the output capacitor C_{S}. When a buck-boost converter operates in discontinuous current mode, its input impedance R_{in} is driven through *SW* 3 by a pulse-width modulated square wave signal of duty cycle δ and frequency f_{s}. When f_{s} is much higher than the input vibration frequency f [16]

$$R_{\mathrm{in}} = \frac{2Lf_{\mathrm{s}}}{\delta^2}. \tag{4}$$

The time evolutions of voltages across C_{R} and R_{L} at the same input acceleration amplitude are shown in Figure 4 with different values of δ when the lossless inductor and the mathematically idealized diodes (i.e., zero voltage drop, near-zero leakage current and zero resistance when conducting) are utilized. After a transient time, V_{L} remains constant at V_{dc} which depends on δ. The power processing circuit is now supplying a DC voltage to the load. $V_{C_{\mathrm{R}}}$ is almost unchanged during operation of the buck-boost converter. Here f is chosen as $f = f_0 = 1/2\pi\sqrt{k_{\mathrm{m}}/m}$. The optimization toward low power consumption of control components is beyond the scope of this paper. However, it should be noted that R_{in} is independent of V_{L}, therefore feedback sensing is not essentially required and the control unit can be further simplified offering power savings. Parameters of the interface circuit are listed in Table 1b, adapted from [16].

To investigate the feasibility of such an introduced topology, diode and inductor losses need to be included. In this paper, we use a piecewise linear diode model which yields a computationally light weight albeit somewhat idealized representation of a diode. The diode losses are thus described by the forward voltage drop V_{D}, the resistance in forward conduction R_{on} and the resistance when off R_{off}. One of the crucial requirements for the energy harvesting system is to be able to operate with low input mechanical power. Hence, diodes with lowest possible losses are preferable. However, the important impact of forward voltage drop on efficiency of

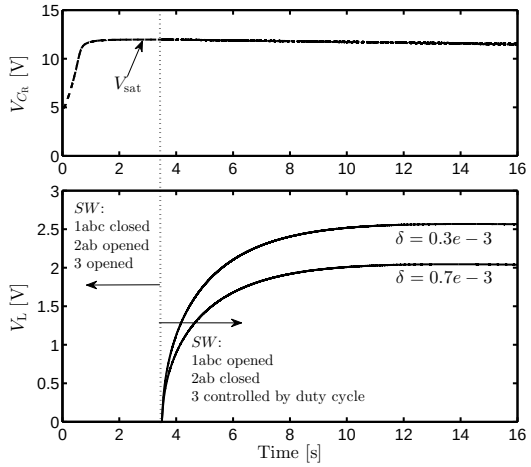

Figure 4: Operation waveforms of voltages across the storage capacitor C_R and the resistive load R_L.

Table 2: Diode parameters.

Parameters	**Values**
Diode voltage drop, V_D	D_H: 0.4 V
	D_L: 26 mV
Conduction resistance, R_{on}	0.5 Ω
Off resistance, R_{off}	10 MΩ

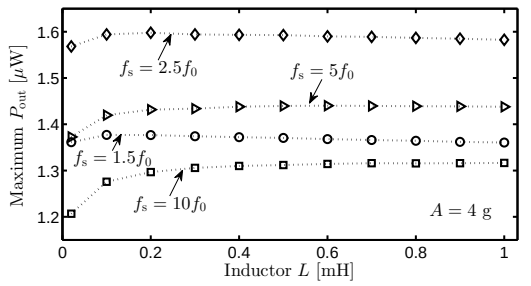

Figure 7: Maximum power versus inductance with different operating frequencies f_s.

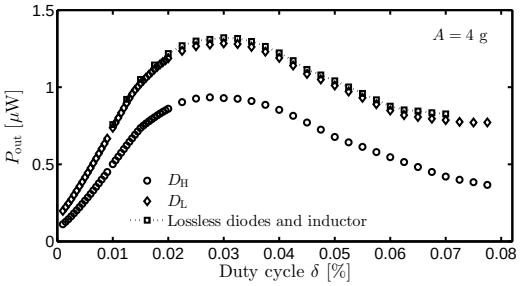

Figure 5: Average power versus duty cycles for different diodes in comparison with ideal case when losses are neglected.

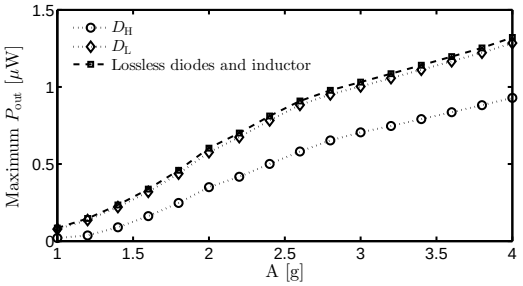

Figure 6: Maximum power versus input acceleration amplitudes.

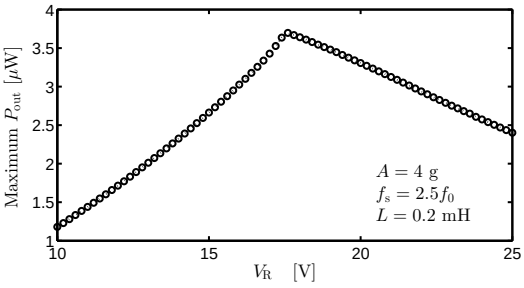

Figure 8: Dependence of maximum power on voltage V_R.

the diodes is not clearly addressed in the literature and is worth further analysis. We choose to consider two different diodes called D_H and D_L as examples for this investigation, in which V_D is the specified value of the real diodes PAD (Pico-Amp Diode) and $SM74611$ respectively. Detail parameters are listed in Table 2.

Figure 5 presents corresponding output power P_{out} when D_H and D_L are used, comparing to the ideal case in that the losses of electronic components are neglected. The simulations show that the power obtained from using D_L is very close to that of the ideal case and both are higher than the other case as expected. The effect of the inductor parasitic resistance is insignificant in this circumstance. The results of maximum power delivered to the load are then expanded to different acceleration amplitudes in Figure 6. In addition, our simulations also predict that the minimum required initial voltage with the use of D_L/D_H are 52 mV/0.79 V, which are about twice V_D of each diode. The maximum harvested power can be further improved with respect

to the switching frequency f_s and the inductance L. Figure 7 shows that about 1.60 μW is achieved with $f_s = 2.5f_0$ and $L = 0.2$ mH. This is an increase of 25.2% in comparison with the case $f_s = 10f_0$ and $L = 150$ μH. These analyses open a room for maximizing the harvested power in future studies, which can be considered as function of f_s, L and even diode parameters.

To investigate the effect of V_{C_R} on the output power, we are now considering a particular circumstance when the transducers are directly coupled to the buck-boost converter (i.e., similar to Figure 3c) and C_R is replaced by a voltage source V_R. The dependence of maximum harvested power on V_R is shown in Figure 8, where $P_{max} \approx 3.7\,\mu$W is obtained with $V_R = 17.5$ V. Here $f_s = 2.5f_0$, $L = 0.2$ mH and $A = 4$ g. These results indicate that, in order to optimize the harvesting system performance, the saturation voltage of the doubler configuration at least needs to reach the optimal bias of the buck-boost converter. In case of $V_{sat} > V_R^{optimal}$, there is an optimal point before saturation at which switches $1a$, $1b$, $1c$, $2a$ and $2b$ should be reverted their states to change the doubler configuration to the buck-boost converter.

4. Conclusion

In this paper, a new power electronic interface for MEMS capacitive energy harvesting was introduced and investigated. This circuit topology enabled to reconfigure the harvesting system from a symmetric doubler circuit to a buck-boost DC-DC converter when the voltage across the storage capacitor reaches an appropriate value. Simulation results showed that the minimum initial bias for efficient operation of the voltage doubler is about twice the voltage drop of diode, while the maximum harvested power strongly depends on the choice of diode, the switching frequency, the duty cycle and the inductance. Essential influence of the voltage V_R for the buck-boost converter configuration was highlighted, raising the requirement to carefully design the harvester so that the saturation voltage of the doubler circuit is at least equal to optimal value of V_R.

Acknowledgment

This work was supported by the Research Council of Norway through Grant no. 229716/E20.

References

[1] Patel S, Park H, Bonato P, Chan L and Rodgers M 2012 *Journal of NeuroEngineering and Rehabilitation* **9** 21 ISSN 1743-0003
[2] Fitzpatrick D 2014 *Implantable Electronic Medical Devices* (Elsevier Science) ISBN 9780124165779
[3] Baronti P, Pillai P, Chook V W, Chessa S, Gotta A and Hu Y F 2007 *Computer Communications* **30** 1655 – 1695 ISSN 0140-3664 Wired/Wireless Internet Communications
[4] Amar A B, Kouki A B and Cao H 2015 *Sensors* **15** 28889–28914 ISSN 1424-8220
[5] Wei X and Liu J 2008 *Frontiers of Energy and Power Engineering in China* **2** 1–13 ISSN 1673-7504
[6] Zheng Q, Shi B, Li Z and Wang Z L 2017 *Advanced Science* **4** 1700029 ISSN 2198-3844 1700029
[7] Zhou Y, Apo D J and Priya S 2013 *Applied Physics Letters* **103** 192909
[8] Fischer A C, Forsberg F, Lapisa M, Bleiker S J, Stemme G, Roxhed N and Niklaus F 2015 *Microsystems & Nanoengineering* **1**
[9] Roundy S, Wright P K and Rabaey J 2003 *Computer Communications* **26** 1131–1144
[10] Yen B C and Lang J H 2006 *IEEE Transactions on Circuits and Systems—Part I: Regular Papers* **53** 288–295
[11] Mitcheson P D, Yeatman E M and Green T C 2006 *Symposium on Design, Test, Integration and Packaging of MEMS/MOEMS* (Stresa, Lago Maggiore, Italy)
[12] de Queiroz A C M and Domingues M 2011 *Circuits and Systems (MWSCAS), IEEE 54th International Midwest Symposium* pp 1–4 ISSN 1548-3746
[13] Dorzhiev V, Karami A, Basset P, Marty F, Dragunov V and Galayko D 2015 *IEEE Electron Device Letters* **36** 183–185 ISSN 0741-3106
[14] Domingues M and de Queiroz A C M 2013 *IEEE International Symposium on Circuits and Systems (ISCAS2013)* pp 2960–2963 ISSN 0271-4302
[15] Wei J, Lefeuvre E, Mathias H and Costa F 2016 *Journal of Physics: Conference Series* **773** 012045
[16] D'hulst R, Sterken T, Puers R, Deconinck G and Driesen J 2010 *IEEE Transactions on Industrial Electronics* **57** 4170 –4177 ISSN 0278-0046